HHS Public Access

Author manuscript

Neuron. Author manuscript; available in PMC 2017 March 02.

Published in final edited form as:

Neuron. 2016 March 2; 89(5): 1000–1015. doi:10.1016/j.neuron.2016.01.043.

NMDA receptor-dependent LTD requires transient synaptic incorporation of Ca^{2+}-permeable AMPA receptors mediated by AKAP150-anchored PKA and calcineurin

Jennifer L. Sanderson[1], **Jessica A. Gorski**[1], and **Mark L. Dell'Acqua**[1,2]

[1]Department of Pharmacology, University of Colorado School of Medicine, 12800 E. 19th Avenue, Aurora, CO 80045

[2]Program in Neuroscience, University of Colorado School of Medicine, 12800 E. 19th Avenue, Aurora, CO 80045

SUMMARY

Information processing in the brain requires multiple forms of synaptic plasticity that converge on regulation of NMDA and AMPA-type glutamate receptors (NMDAR, AMPAR), including long-term potentiation (LTP) and depression (LTD) and homeostatic scaling. In some cases, LTP and homeostatic plasticity regulate synaptic AMPAR subunit composition to increase the contribution of Ca^{2+}-permeable receptors (CP-AMPARs) containing GluA1 but lacking GluA2 subunits. Here, we show that PKA anchored to the scaffold protein AKAP150 regulates GluA1 phosphorylation and plays a novel role controlling CP-AMPAR synaptic incorporation during NMDAR-dependent LTD. Using knock-in mice that are deficient in AKAP-anchoring of either PKA or the opposing phosphatase calcineurin, we found that CP-AMPARs are recruited to hippocampal synapses by anchored PKA during LTD induction but are then rapidly removed by anchored calcineurin. Importantly, blocking CP-AMPAR recruitment, removal or activity interferes with LTD. Thus, CP-AMPAR synaptic recruitment is required to transiently augment NMDAR Ca^{2+} signaling during LTD induction.

INTRODUCTION

LTP and LTD at excitatory synapses are thought to underlie experience-dependent learning and memory. These synaptic plasticity mechanisms are best characterized at hippocampal CA1 synapses, where they are frequently altered in animal models of human neurodevelopmental, neuropsychiatric, and neurological disorders. The most prevalent forms of LTP and LTD are induced by Ca^{2+} influx through postsynaptic NMDARs and are

*Correspondence: mark.dellaqua@ucdenver.edu.

AUTHOR CONTRIBUTIONS

MLD and JLS designed the research. JLS performed electrophysiology experiments. JAG performed subcellular fractionation, immunoblotting, and Golgi staining. JLS and MLD wrote manuscript with input from JAG.

expressed by long-lasting increases or decreases, respectively, in the synaptic localization and function of AMPARs (Collingridge et al., 2010; Huganir and Nicoll, 2013).

AMPARs are tetrameric assemblies of GluA1-GluA4 subunits and, except very early in postnatal development, the majority of receptors at CA1 synapses are composed of GluA1/2 or GluA2/3, with GluA2 decreasing conductance and preventing Ca^{2+} influx (Lu et al., 2009; Stubblefield and Benke, 2010). However, smaller numbers of high-conductance, Ca^{2+}-permeable GluA1 homomeric AMPARs (CP-AMPARs) are also present, primarily in extrasynaptic and intracellular locations from where they can be recruited to synapses by some LTP-inducing stimuli (Guire et al., 2008; Lu et al., 2007; Plant et al., 2006; Qian et al., 2012; Rozov et al., 2012; Yang et al., 2010)(but see (Adesnik and Nicoll, 2007; Gray et al., 2007)). CP-AMPARs are also recruited to hippocampal and cortical synapses during certain forms of homeostatic plasticity (Goel et al., 2011; Kim and Ziff, 2014; Soares et al., 2013; Sutton et al., 2006; Thiagarajan et al., 2005), as well as in response to seizures and ischemia (Liu and Zukin, 2007). In addition, CP-AMPARs are recruited to synapses in the amygdala during fear learning (Clem and Huganir, 2010) and in the nucleus accumbens and ventral tegmentum in models of drug addiction (Bellone et al., 2011; McCutcheon et al., 2011). Nonetheless, the signaling mechanisms regulating synaptic AMPAR subunit composition are still not well understood.

Phosphorylation of S845 in the GluA1 C-terminal tail by the cAMP-dependent protein kinase (PKA) can prime AMPARs for synaptic insertion during LTP in response to subsequent NMDAR-Ca^{2+}activation of Ca^{2+}/calmodulin-dependent protein kinases I and II (CaMKII) and PKC (Esteban et al., 2003; Guire et al., 2008; Hu et al., 2007; Oh et al., 2006; Sun et al., 2005; Yang et al., 2008). In contrast, during LTD the Ca^{2+}-activated protein phosphatase-2B/calcineurin (CaN) dephosphorylates S845 and promotes AMPAR removal from synapses and endocytosis (Beattie et al., 2000; Ehlers, 2000; Lee et al., 2000; Lee et al., 1998; Mulkey et al., 1994; Sanderson et al., 2012). Previous studies also indicate that S845 phosphorylation plays a key role in regulating CP-AMPAR abundance, trafficking, and synaptic incorporation (Esteban et al., 2003; He et al., 2009; Man et al., 2007; Qian et al., 2012); GluA1 S845A knock-in mice possess fewer GluA1 homomers, exhibit impaired PKA regulation of LTP, and have deficits in LTD in the hippocampus (He et al., 2009; Hu et al., 2007; Lee et al., 2003; Lee et al., 2010; Qian et al., 2012). In addition, recent studies have implicated CP-AMPARs, S845 phosphorylation, PKA, and CaN in homeostatic plasticity mechanisms that scale-up synaptic strength in response to decreased neuronal firing (Diering et al., 2014; Goel et al., 2011; Kim and Ziff, 2014).

Given all of the above studies implicating S845 in plasticity regulation, it may seem surprising that a recent biochemical study found that steady-state levels of S845 phosphorylation are very low, even in synaptic fractions (Hosokawa et al., 2015). However, an inherent limitation of even the most quantitative bulk phosphorylation measurements is that they cannot report rapid, localized changes in phosphorylation that occur within the confines of receptor-scaffolded kinase/phosphatase signaling complexes. In particular, PKA and CaN are targeted to GluA1 through binding to a common scaffold protein, A-kinase anchoring protein (AKAP) 79/150 (human79/rodent150; also known as AKAP5)(Woolfrey and Dell'Acqua, 2015). Inhibition of AKAP-PKA anchoring, like GluA1 S845A mutation,

prevents PKA enhancement of LTP (Lu et al., 2007; Zhang et al., 2013). However, somewhat paradoxically, inhibition of AKAP-PKA signaling also interferes with LTD that relies on S845 dephosphorylation and AMPAR removal by AKAP-anchored CaN (Jurado et al., 2010; Kameyama et al., 1998; Lu et al., 2008; Sanderson et al., 2012; Snyder et al., 2005; Tunquist et al., 2008).

While it is not known if CP-AMPAR regulation is required for LTD, our previous characterization of AKAP150ΔPIX knock-in mice that are selectively deficient in CaN anchoring, due to disruption of a PxIxIT-type CaN docking motif, provided important insights. We found that AKAP-CaN signaling dephosphorylates GluA1 S845 and limits synaptic incorporation of CP-AMPARs to constrain LTP and promote LTD (Sanderson et al., 2012). These previous findings suggested that phosphorylation-regulated CP-AMPAR recruitment to synapses may also occur during LTD, but how inhibition of either AKAP-PKA or -CaN signaling and either increases or decreases in S845 phosphorylation all result in impaired LTD remained unclear. Here, we address this conundrum by using a combination of molecular genetic, pharmacological and electrophysiological approaches to uncover a novel mechanism where phosphorylated GluA1 CP-AMPARs are transiently recruited to synapses *during* NMDAR-dependent LTD induction before signaling their own removal and being dephosphorylated. Through analysis of AKAP150 mutant mice, we demonstrate that CP-AMPARs are recruited to synapses by anchored PKA during LTD induction but are then rapidly removed by anchored CaN, and that blocking either CP-AMPAR activity, recruitment or removal interferes with LTD. Our findings of PKA-dependent synaptic recruitment of CP-AMPARs during LTD reveal remarkable and unexpected parallels with some previously proposed LTP and homeostatic plasticity mechanisms, thus further underscoring the complex signaling crosstalk underlying these distinct, yet interrelated, forms of synaptic regulation.

RESULTS

Genetic disruption of PKA anchoring in AKAP150ΔPKA knock-in mice decreases the amount of type-II PKA in the PSD but does not impact basal transmission at hippocampal CA1 synapses

To further characterize the role of AKAP-PKA signaling in LTD, we recently generated PKA-anchoring deficient AKAP150 ΔPKA knock-in mice by internally deleting 10 amino acids within the PKA-RII subunit binding amphipathic α-helix near the AKAP C-terminus (Figure 1A)(Murphy et al., 2014). This 150ΔPKA mutation has the advantage of being more specific than a larger 36 amino acid C-terminal truncation in previously characterized PKA-anchoring deficient AKAP150 D36 mice, which also removed the modified leucine-zipper motif that interacts with L-type Ca^{2+} channels (Lu et al., 2007; Oliveria et al., 2007). In agreement with our recent characterization of hippocampal neurons from 150ΔPKA mice showing normal AKAP150 localization but reduced PKA-RII localization in dendritic spines (Murphy et al., 2014), subcellular fractionation and immunoblotting of hippocampal tissue revealed normal distribution of AKAP150 (Figure 1B) but a significant reduction in the amount of PKA-RIIα present in crude PSD fractions from ~2 week-old 150ΔPKA mice compared to WT (Figure 1B, C; TxP: WT 0.72±0.03, ΔPKA 0.34±0.09 normalized to WT

whole-cell extracts (WE) for, n=3, **p=0.0069 by unpaired t-test). However, PKA-RIIα expression levels were normal in whole-cell extracts (WE) as well as in fractions containing both pre- and postsynaptic membranes (P2) and cytosol and microsomal membranes (S2). In addition, the expression levels and distributions of other AKAP-associated proteins (CaNA, GluA1, PSD-95 family MAGUK scaffolds, N-cadherin) were unchanged (Figure 1B–D). Thus, as designed, the 150ΔPKA mutation specifically reduces postsynaptic PKA localization.

While previous studies of AKAP150 knockout and D36 mice also documented decreased PKA-RII in the PSD (Lu et al., 2007; Weisenhaus et al., 2010), they found that at ~2 weeks of age both mouse strains exhibited substantially elevated dendritic spine numbers in the CA1 stratum radiatum. These increases in spine density were accompanied by sizeable increases in the frequency, but not amplitudes, of spontaneous miniature excitatory postsynaptic currents (mEPSC), indicating increases in the number, but not strength, of excitatory synapses on CA1 neurons (Lu et al., 2011). However, imaging of Golgi-stained CA1 neurons from 150ΔPKA mice showed only a very slight increase in spine density relative to WT (Figure 1E,F: WT 1.85±0.07, ΔPKA 2.06±0.07 spines/μm dendrite, n=29–39 dendrite segments, *p=0.042 by unpaired t-test). Likewise, whole-cell recording from CA1 neurons in acute hippocampal slices prepared from 150ΔPKA mice revealed no significant changes in the amplitudes or frequency of mEPSC (Figure S1A–E) or spontaneous EPSC (sEPSC) events, which are comprised of mEPSC plus action potential evoked events (Figure 2A–C; sEPSC amplitude: WT 15.2±1.2, ΔPKA 14.4±0.7 pA, p=0.66; see also Figure S1C; sEPSC frequency: WT 0.37±0.5, ΔPKA 0.35±0.1 Hz, p=0.83 by unpaired t-test, n=21). Although, there is a trend (p=0.06) toward slightly increased mean mEPSC amplitude (Figure S1A) and a small rightward-shift in the cumulative distribution mEPSC amplitudes for 150ΔPKA mice (Figure S1B). Previous studies found that CA1 neurons from juvenile AKAP150 knockout and D36 mice also exhibit increased basal GABAergic inhibitory synaptic transmission (Lu et al., 2011), but our characterization of 150ΔPKA mice found no such changes in either the amplitudes or frequency of miniature (mIPSC; Figure S1F–J) or spontaneous inhibitory postsynaptic currents (sIPSC)(Figure 2D–F; sIPSC amplitude: WT 69±9, ΔPKA 66±8 pA, p=0.79; see also Figure S1H; sIPSC frequency: WT 7.4±0.8, ΔPKA 7.6±0.9 Hz, p=0.89 by unpaired t-test, n=13–18). Thus, overall levels of basal excitatory and inhibitory synaptic input onto CA1 neurons are essentially normal in juvenile 150ΔPKA mice.

Consistent with these observations of normal basal synaptic transmission, when stimulating the Schaefer collateral (SC) inputs from CA3 and recording evoked responses in 150ΔPKA CA1 neurons, we also found no changes in AMPA/NMDA EPSC amplitude ratios, which we measured as the ratio of peak amplitudes of either of the AMPA EPSC fast inward (−65 mV holding potential) or outward (+40 mV holding potential) components to the slow outward NMDA EPSC component (+40 mV holding potential, measured 70 ms after peak) (Figure 2G–I; −65AMPA/+40NMDA: WT 3.7±0.5, ΔPKA 3.6±0.6, p=0.99; +40AMPA/+40 NMDA: WT 1.6±0.2, 1.8±0.3 ΔPKA, p=0.35 by unpaired t-test, n=9–10). Likewise, extracellular recordings of CA1 field excitatory postsynaptic potential (fEPSP) input/output relationships across a range of stimulus intensities and paired-pulse ratios across a range of

inter-stimulus intervals revealed no changes in basal postsynaptic AMPAR activity or presynaptic function in 150ΔPKA mice, respectively (Figure 2J–L).

Basal GluA1 Ser845 phosphorylation is decreased but synaptic AMPAR subunit composition is unchanged in AKAP150ΔPKA mice

Our previous characterization of CaN-anchoring deficient AKAP150 ΔPIX mice also found no changes in basal excitatory or inhibitory transmission but did uncover basal increases in GluA1 S845 phosphorylation and CP-AMPAR activity at CA1 synapses (Sanderson et al., 2012). Thus, we next examined whether basal regulation of GluA1 phosphorylation and synaptic AMPAR subunit composition were altered in 150ΔPKA mice. Immunoblotting revealed ~40–45% reductions in S845 phosphorylation for both hippocampal whole-cell extracts and P2-synaptic fractions prepared from 150ΔPKA versus WT mice (Figure 3A, B; S845/GluA1 normalized to WT on the same blots: WE 0.54±0.01, **p=0.009; P2 0.61±0.03, ***p=0.0002; S2 0.80±0.12, p=0.16; one-sample t-test, n=5). CP-AMPARs are sensitive to block of outward currents at positive holding potentials by intracellular polyamines, leading to pronounced inward-rectification seen on current versus voltage (I/V) plots (Rozov et al., 1998). However, I/V plots for evoked AMPA EPSCs measured at a range of holding potentials (Figure 3C) and calculation of −65 mV/+40 mV EPSC rectification indices (RI) revealed essentially linear I/V relationships with little evidence of inward rectification in either WT or 150ΔPKA mice (Figure 3D; +65/+40 AMPA RI: WT 2.3±0.3, ΔPKA 2.0±0.2, p=0.38 unpaired t-test, n=9–10).

LTP expression is inhibited by antagonism of CP-AMPARs in 2 but not 3 week-old WT mice

As mentioned above, CP-AMPARs can be recruited to synapses during certain forms of plasticity, but the involvement of CP-AMPARs in LTP at CA1 synapses remains controversial, with a number of published studies either supporting (Guire et al., 2008; Lu et al., 2007; Plant et al., 2006; Yang et al., 2010) or refuting (Adesnik and Nicoll, 2007; Gray et al., 2007) CP-AMPAR synaptic recruitment in LTP. One variable between studies is the type and strength of the LTP inducing stimuli; however, another significant variable may be the developmental age of the animals and the accompanying differences in developmental plasticity of LTP mechanisms. For example, several studies using mutant mice found that GluA1, S845 phosphorylation, PKA, CP-AMPARs, and AKAP150 all regulate LTP induced by brief, high frequency stimuli, as well as enhancement of LTP by β-adrenergic receptors, in slices prepared from young adult animals (~6–8 weeks and older)(Lee et al., 2003; Lu et al., 2007; Qian et al., 2012; Zamanillo et al., 1999; Zhang et al., 2013). However, findings become much more variable with respect to these same players and LTP in juvenile animals, especially in the range of ~2–3 weeks of age when the hippocampus is still undergoing synaptogenesis and other developmental changes (Adesnik and Nicoll, 2007; Granger et al., 2013; Gray et al., 2007; Jensen et al., 2003; Lu et al., 2007; Plant et al., 2006; Sanderson et al., 2012; Yang et al., 2010). Thus, here we used a single, standard high frequency stimulus (HFS: 1×100Hz, 1s) to induce LTP in WT mice between ~2 and 3 weeks of age and then compared the impact of adding the CP-AMPAR-selective polyamine antagonist IEM1460 on the level of LTP expression. In mice ≤ 2 weeks of age (P11-14), addition of IEM1460 immediately after induction consistently suppressed LTP expression (Figure 3E, t=50–56

min: F(1,52) 192.8,***p<0.0001, n=5–11, by two-way ANOVA; Figure 3G, t=60 min %baseline: WT(2 wks) 129±4, ***p<0.0001 to pre-LTP, n=11; WT(2 wks)+IEM 80±2, **p=0.0033 to pre-LTP, ***p<0.0001 to WT(2 wks), n=5; unpaired t-tests). In contrast, IEM1460 addition had essentially no impact on LTP expression in animals closer to 3 weeks of age (P17-21) (Figure 3F; t=50–56 min: F(1,40) 1.78, p=0.19, n=5–7, by two-way ANOVA; Figure 3G, t=60 min %baseline: WT(3 wks) 139±14, *p=0.021 to pre-LTP, n=7; WT(3 wks)+IEM 134±5, ***p=0.0001 to pre-LTP, p=0.76 to WT(3 wks), n=5; unpaired t-tests).

LTP is expressed at normal levels in 2 week-old AKAP150ΔPKA mice but is insensitive to CP-AMPAR antagonism

We next determined whether LTP was altered in ≤2 week-old 150ΔPKA mice and, surprisingly, found that the level of LTP expression was normal relative to WT (Figure 3H; t=50–56 min: F(1,76) 0.84, p=0.36, n=10–11, by two-way ANOVA; Figure 3J, t=60 min %baseline: 150ΔPKA 133±9, **p=0.0033 to pre-LTP, n=10, p=0.69 to WT(2 wks); unpaired t-tests). However, unlike WT mice, expression of LTP in ≤ 2 week-old 150ΔPKA mice was now completely insensitive to IEM1460 (Figure 3I; t=50–56 min: F(1,56) 2.83, p=0.098, n=6–10, by two-way ANOVA; Figure 3J, t=60 min %baseline: 150ΔPKA+IEM 155±15, **p=0.0034 to pre-LTP baseline, n=6, p=0.21 to 150ΔPKA; unpaired t-tests). Thus, it appears that a shift to LTP using only GluA2-containing AMPARs occurred in P11-14 150ΔPKA mice, perhaps similar to that which occurs in WT mice just a few days later in development. This shift to LTP expression by solely GluA2-containing receptors could be necessitated by decreased S845 phosphorylation in 150ΔPKA mice (Figure 3A,B) leading to an inability to mobilize CP-AMPARs to the synapse, but could also be related to somewhat precocious postsynaptic maturation, as suggested by a trend toward slightly increased mEPSC amplitude in 150ΔPKA mice (Figure S1A,B).

LTD is impaired in AKAP150Δ PKA mice

Since AKAP-PKA signaling and GluA1-Ser845 phosphorylation are also implicated in LTD, we next examined LTD induced by prolonged low frequency stimulation (LFS; 1 Hz, 15 min) in ≤ 2 week-old 150ΔPKA mice. Consistent with studies of AKAP150 D36 mice (Lu et al., 2008), we found that LTD was still detectable for 150ΔPKA mice but was significantly reduced compared to WT (Figure 3K; t=70–80 min: F(1,90) 70.39, ***p<0.0001, n=8–9, by two-way ANOVA; Figure 3M, t=80 min %baseline: WT 70±4, ***p<0.0001 to pre-LTD, n=9; 150ΔPKA 88±5, *p=0.014 to pre-LTD, $^{\#\#}$p=0.006 to WT, n=8; unpaired t-tests). Our previous studies revealed that antagonism of CP-AMPARs with IEM1460 post-induction could partially rescue LTD in 150ΔPIX mice but had no impact in WT, indicating that LTD impairment in 150ΔPIX mice was due to an inability to remove CP-AMPARs from synapses (Sanderson et al., 2012). However, here when we added IEM1460 (70 μM) post-induction to slices from WT or 150ΔPKA mice we observed no significant impact on the ultimate level of LTD expression for either genotype (Figure 3L; t=70–80 min: WT+IEM F(1,84) 2.5, p=0.12 to WT, n=7; 150ΔPKA+IEM F(1,90) 0.053, p=0.82 to 150ΔPKA, n=9, by two-way ANOVA; Figure 3M, t=80 min %baseline: WT+IEM 75.7±8.9, *p=0.024 to pre-LTD, p=0.54 to WT, n=9; 150ΔPKA+IEM 88.6±4.8, *p=0.040 to pre-LTD baseline, p=0.88 to 150ΔPKA, n=8; unpaired t-tests). These IEM1460 results

indicate that reduced LTD in 150ΔPKA mice is not due to a failure to remove CP-AMPARs as in 150ΔPIX mice, not an unexpected finding because ΔPIX increases, while ΔPKA decreases, phospho-S845 levels. Thus, paradoxically, either increasing or decreasing S845 phosphorylation relative to WT is associated with impaired LTD.

Antagonist application during induction reveals a novel role for CP-AMPAR activity in NMDAR-dependent LTD

In order to reconcile these seemingly incongruent findings, we next explored whether the LTD deficit in 150ΔPKA mice could instead be due to a failure to recruit CP-AMPARs to participate in postsynaptic Ca^{2+} signaling *during* LTD induction. We were limited to adding IEM1460 after LTD or LTP induction because this compound can also partially inhibit NMDARs at the concentration we used. Thus, instead we continuously applied another antagonist NASPM to WT slices at a dose (20 μM) that blocks CP-AMPARs but not NMDARs (Lu et al., 2007)(see also Figure S2) and found that LTD was still present but now reduced compared to control. (Figure 4A; t=70–80 min: WT+NASPM F(1,72) 28.3, ***p<0.0001 to WT control, n=9, by two-way ANOVA; Figure 4G, t=80 min %baseline: 85±7, *p=0.029 to pre-LTD, $^{\#}$p=0.044 to WT control, n=5, unpaired t-tests). In contrast, continuous NMDAR antagonism with the open-channel blocker MK801 (10 μM) completely inhibited LTD, confirming previous studies showing that CA1 LTD induction requires NMDAR Ca^{2+} influx (Babiec et al., 2014; Coultrap et al., 2014; Dudek and Bear, 1992; Mulkey and Malenka, 1992; Raymond et al., 2003; Sanderson et al., 2012)(but see (Nabavi et al., 2013))(Figure 4B, t=70–80 min: WT+MK801 F(1,88) 58.4, ***p<0.0001 to WT control, n=7, by two-way ANOVA; Figure 4G, t=80 min %baseline: 97±9, p=0.36 to pre-LTD, **p=0.0097 to WT control, n=7, unpaired t-tests). Strikingly, when NASPM was washed out after induction, LTD expression was completely inhibited and a variable amount of synaptic potentiation was observed instead (Figure 4C; complete washout estimated by ~20 min post-LFS (gray bar); t=70–80 min: WT+NASPM washout F(1,96) 84.2 ***p<0.0001 to WT control, n=9, by two-way ANOVA; Figure 4G, t=80 min %baseline: 123±14, p=0.06 to pre-LTD baseline, $^{\#\#}$p=0.002 to WT control, n=9, unpaired t-tests). This variable potentiation upon NASPM washout was prevented by co-application of MK801 to block NMDARs (Figure 4C; t=70–80 min: WT+NASPM washout+MK801 F(1,78) 14.5 ‡‡‡p=0.0003 to WT+NASPM washout, F(1,78) 75.7, ***p<0.0001 to WT control, F(1,54) 7.1 $^{\#}$p=0.01 to WT+NASPM (no washout), n=6, by two-way ANOVA; Figure 4G, t=80 min %baseline: 99±7, p=0.33 to pre-LTD, $^{\#\#}$p=0.0013 to WT control, n=6, unpaired t-tests). Some variability in the levels of depression or potentiation seen with NASPM and MK801 likely reflects variability in the levels and times of onset of use-dependent open-channel block or unblock (for NASPM washout) due to variable slice perfusion. Nonetheless, it is apparent that NASPM washout after LTD induction resulted in significantly greater inhibitory impact than continuous NASPM application (Figure 4C, F(1,72) 23.6 $^{\#\#\#}$p<0.0001 by two-way ANOVA; Figure 4G, †p=0.038 by unpaired t-test). These impacts of MK801 and NASPM, taken together with insensitivity to IEM1460 post-induction, indicate that NMDAR signaling during LTD induction recruits CP-AMPARs to the synapse and then Ca^{2+} signaling by the recruited receptors helps determine the subsequent level of LTD expression before triggering their own removal.

CP-AMPARs are recruited to synapses during LTD induction by AKAP150-PKA signaling before being rapidly removed by AKAP150-CaN signaling

Intriguingly, the reduced level of LTD expression seen in WT slices with continuous NASPM application (Figure 4A) is very similar to that observed in 150ΔPKA slices under control conditions (Figure 3K), thus we next examined whether LTD-induced CP-AMPAR recruitment is regulated by PKA and CaN. Consistent with previous studies (Lu et al., 2008), acute application of the PKA-selective inhibitor H89 inhibited LTD in WT slices (Figure 4D; t=70–80 min: WT+NASPM washout+H89 F(1,78) 200 ***p<0.0001 to WT control; F(1,54) 31.9 $^{\#\#\#}$p<0.0001 to WT+NASPM (no washout) by 2-way ANOVA; Figure 4G, t=80 min %baseline: 102±4, p=0.29 to pre-LTD, $^{\#\#}$p<0.0001 to WT control, n=6, unpaired t-tests) and, importantly, also prevented synaptic potentiation upon NASPM washout (compare Figure 4D to 4C, t=70–80 min F(1,78) 8.9 ‡‡p<0.0037 by 2-way ANOVA). Furthermore, NASPM washout did not result in any AMPAR potentiation in 150ΔPKA slices (compare Figure 4C to 4E, t=70–80 min: ΔPKA+NASPM washout F(1,84) 34.8 ‡‡‡p<0.0001 to WT +NASPM washout, n=7, by 2-way ANOVA), but instead reduced LTD was still observed (Figure 4E, t=70–80 min: F(1,84) 28.8 ***p<0.0001 to WT control by 2-way ANOVA; Figure 4G, t=80 min %baseline: 86±5, **p=0.007 to pre-LTD, *p=0.012 to WT control, unpaired t-tests). This reduced LTD in 150ΔPKA+NASPM was no different from that seen for continuous NASPM application to WT slices (Compare Figure 4E to 4A, t=70–80 min: F(1,60) 18.9 p=0.76 to WT+NASPM (no washout), by 2-way ANOVA) or for 150ΔPKA slices under control conditions (compare Figure 4E to 3K, t=70–80 min: F(1,78) 3.6 p=0.062 by 2-way ANOVA). Consistent with our previous work showing that post-LFS IEM1460 application rescues LTD in 150ΔPIX mice (Sanderson et al., 2012), synaptic depression was evident initially after LFS in 150ΔPIX slices in the presence of NASPM, but as the drug was washed out and CP-AMPARs became unblocked this rescue of depression was lost and ultimately no significant LTD was maintained nor was any washout-associated potentiation observed (Figure 4F; t=70–80 min: ΔPIX+NASPM washout F(1,96) 157.8 ***p<0.0001 to WT control, F(1,72) 12.9 ***p=0.0006 to WT+NASPM (no washout), F(1,96) 25.9 ‡‡‡p<0.0001 to WT+NASPM washout, n=9, by 2-way ANOVA; Figure 4G, t=80 min %baseline: 96±3, p=0.14 to pre-LTD, $^{\#\#\#}$p<0.0001 to WT control, unpaired t-tests). Overall, these pharmacology studies are consistent with AKAP150-PKA signaling being required for CP-AMPAR recruitment during LTD induction and then AKAP150-CaN signaling being required for subsequent removal.

To further examine PKA and CaN regulation during LTD, we performed whole-cell recording experiments to more directly measure CP-AMPAR activity. First, we recorded inward AMPA EPSCs (at −65 mV) and induced LTD using a protocol pairing depolarization of the postsynaptic CA1 neuron to −30 mV with presynaptic stimulation of SC inputs at 1 Hz for 6 min (Figure 5A,B). This LFS pairing-protocol very reliably induced substantial LTD in WT neurons (Figure 5B; t=30 min %baseline: 74±7, **p=0.005 to pre-LTD by unpaired t-test, n=9–10) but, as expected, failed to induce any significant LTD in either 150ΔPKA (Figure 5A; t=30–33 min: F(1,64) 21.7 ***p<0.0001 to WT by 2-way ANOVA, n=9; Figure 5B, t=30 min %baseline: 112±13, p=0.38 to pre-LTD by unpaired t-tests, $^{\#}$p<0.05 to WT by one-way ANOVA, n=9–10) or 150ΔPIX neurons (Figure 5A; t=30–33 min: F(1,44) 38.9 ***p<0.0001 to WT by 2-way ANOVA, n=4), the later of which

displayed variable, but significant, synaptic potentiation (Figure 5B; t=30 min %baseline: 134±23, *p=0.049 to pre-LTD baseline by unpaired t-tests, $^{\#}$p<0.05 to WT by one-way ANOVA, n=4–6). As a control for the input specificity of LTD induction, we also monitored sEPSC amplitudes before and after LTD induction and found no significant changes for any genotype, thus ruling out contributions from changes in overall synaptic activity to the observed LTD phenotypes (WT 5.7±7.4%, n=9, p=0.46; ΔPKA 5.9±6.0%, n=13, p=0.34; ΔPIX 7.7±4.4%, n=5, p=0.15; one-sample t-tests).

To monitor changes in synaptic AMPAR subunit composition, we repeated these LTD experiments recording both inward (−65 mV) and outward EPSCs (+60 mV) at specific time points before, during (3 min into 6 min LFS-pairing), and 1, 5, and 10 min post-LTD induction (Figure 5C–E; 5 and 10 min-post time-points combined for analysis). We then calculated AMPAR rectification index (RI) as the ratio of inward to outward (−65/+60) EPSC peak amplitude. Due to strong inward rectification in 150ΔPIX neurons, outward EPSCs were measured at +60 mV (instead of +40 mV as in Figure 3B and (Sanderson et al., 2012)) to increase outward current amplitude, allowing for more accurate measurement; however, a −65/+60 RI will under-report the degree of inward rectification compared to a −65/+40 RI because some relief from intracellular polyamine block occurs as depolarization increases (Rozov et al., 1998). Nonetheless, in WT neurons we observed a significant increase in AMPAR RI during LTD induction that rapidly returned to pre-induction levels from 1 min post-induction onward (Figure 5F; RI: Before 1.4±0.1; During LFS 2.4±0.3 **p<0.01 to Before by one-way ANOVA; 1 min 1.4±0.2; 5–10 min 1.4±0.2; n=9–15). In 150ΔPKA neurons we observed a very small, transient increase in RI during LFS-induction of LTD but this increase was significantly reduced compared to WT indicating a deficit in CP-AMPAR recruitment (Figure 5G; RI: Before 1.2±0.1; During LFS 1.7±0.1 **p<0.01 to Before by one-way ANOVA, ‡p=0.022 to WT During LFS by unpaired t-test; 1 min 1.2±0.1; 5–10 min 1.4±0.1; n=10–15). In agreement with our previous work (Sanderson et al., 2012), AMPAR RI in 150ΔPIX neurons was already significantly increased relative to WT before LTD induction (Figure 5H; RI: Before 2.6±0.3 $^{\#\#\#}$p<0.0001 to WT by unpaired t-test; n=11), and increased RI was persistently maintained during and after LTD induction, consistent with a failure to remove synaptic CP-AMPARs (Figure 5H; RI: During LFS 4.1±1.0; 1 min 3.4±1.2; 5–10 min 3.0±0.7; n=9–13).

While the majority of the peak amplitude of the outward +60 mV EPSC is contributed by AMPARs, due to their faster kinetics, some contamination of this peak amplitude by the rising phase of the slower NMDAR component is present. To control for any confounding impact of contaminating NMDAR current, we performed two additional analyses. First, we measured the slow outward NMDA EPSC component at 50 ms after the peak and found that NMDAR activity in WT, 150ΔPKA, and 150ΔPIX neurons showed similar transient depression and then subsequent recovery during and after LFS (Figure 5I: no significant differences across genotypes at any time point by one-way ANOVA, p>0.05). In addition, direct inhibition of NMDARs with the competitive antagonist APV (50 μM) in WT slices in separate experiments under baseline recording conditions did not significantly change RI values (Before APV 1.2±0.2; after APV 1.4±0.2; n=5; p=0.11 by paired t-test). Thus, changes in NMDAR contributions to the +60 mV EPSC peak cannot account for the distinct RI changes observed for WT compared to ΔPKA and ΔPIX during LFS. Second, we

measured the relative degree of depression of the initial slope of the inward versus outward EPSC as independent measures of AMPAR activity and rectification that are not contaminated by the slower NMDAR component (Figure 5J–K)(Adesnik and Nicoll, 2007). Consistent with increased AMPAR rectification, in WT neurons we saw greater depression of outward than inward EPSC slope during LFS compared to before induction (Figure 5J; +60: 0.38±0.08, −65: 0.6±0.1, *p=0.013 by paired t-test, n=10; Figure 5K; Δ−65/Δ+60: 1.9±0.3, *p=0.013 to 1.0 by one-sample t-test). Importantly, this differential change in outward versus inward EPSC slope during LFS was not observed in ΔPKA or ΔPIX neurons that exhibit impaired LTD (Figure 5J; ΔPKA +60: 0.8±0.2, −65: 0.8±0.1, p=0.99 by paired t-test, n=10; ΔPIX +60: 0.7±0.2, −65: 0.8±0.2, p=0.68 by paired t-test, n=9; Figure 5K, ΔPKA Δ−65/Δ+60: 1.0±0.2, p=0.95 by one-sample t-test; ΔPIX Δ−65/Δ+60: 1.1±0.3, p=0.63 by one-sample t-test; $^{\#}$p<0.05 to WT by one-way ANOVA).

Finally, by applying NASPM (20 μM) to block CP-AMPARs during LFS in WT neurons, we were able to prevent RI increase (Figure 6A,C; RI: Before 1.5±0.2; NASPM During LFS 1.7±0.2, p=0.31 by paired t-test to Before, reduced relative to Control During LFS $^{\#}$p<0.05 by one-way ANOVA; n=8) and depression of both outward and inward AMPAR EPSC slope measured 3 min after initiation of LFS (Figure 6E; NASPM +60: 1.0±0.2, −65: 1.1±0.1, p=0.77 by paired t-test, n=8; Figure 6F; NASPM Δ−65/Δ+60: 1.0±0.2, p=0.97 to 1.0 by one-sample t-test; reduced relative to Control $^{\#}$p<0.05 by one-way ANOVA). As a control, we established that application of NASPM did not inhibit pharmacologically-isolated NMDAR EPSCs, even after ~8 min, when recorded at a holding potential of −30 mV (i.e. same as LFS-LTD induction; Figure S2). In contrast, APV application, to acutely block NMDARs and isolate the outward AMPAR EPSC during LFS, still allowed for a significant RI increase (Figure 6B,C; RI: Before 1.2±0.2, APV During LFS 1.8±0.2; ***p=0.0008 to Before by paired t-test; n=8) and greater relative depression of outward versus inward EPSC slope (Figure 6E; APV +60: 1.1±0.1, −65: 0.8±0.1, *p=0.022 by paired t-test, n=8; Figure 6F; NASPM Δ−65/Δ+60: 1.50±0.2, *p=0.029 to 1.0 by one-sample t-test). However, consistent with NMDAR activity being required for CP-AMPAR recruitment and overall LTD induction, the RI increase observed during LFS in APV was reduced relative to WT controls (Figure 5C; $^{\#}$p<0.05 by one-way ANOVA), and the relative depression of EPSC outward slope was not accompanied by net depression of inward slope as in controls (Figure 6E; APV −65 mV p=0.23 to 1.0 by one-sample t-test; Control −65 mV *p=0.016 reduced relative to 1.0 by one-sample t-test). Similar results were obtained when MK801 was applied during LFS delivery (Figure S3A,C–D). Importantly, measurements of the slow outward NMDAR EPSC component 50 ms after peak during LFS revealed equivalent NMDAR depression relative to before LFS in the presence of NASPM compared to controls (Figure 6D; NASPM 0.33±0.07, Control 0.25±0.04, p>0.05 by one-way ANOVA) and confirmed that APV or MK801 application effectively further inhibited NMDAR activity (Figure 6D; APV 0.09±0.02, *p<0.05 to both Control and NASPM by one-way ANOVA; Figure S3B). Once again, changes in NMDAR contribution to the +60 mV EPSC component cannot account for the differential impacts of NASPM, APV or MK801 on AMPAR rectification measurements during LFS. Overall, these pharmacologic treatments and multiple, independent data analyses indicate that CP-AMPARs are transiently recruited and then removed from synapses during the LTD induction stimulus in WT mice and that deficits in

LTD in AKAP150 ΔPKA and ΔPIX mice are accompanied by failures to recruit to or remove CP-AMPARs from synapses, respectively.

DISCUSSION

Our present findings demonstrate that AKAP-anchored PKA is required during LTD induction to facilitate NMDAR-dependent recruitment of CP-AMPARs to participate in postsynaptic Ca^{2+} signaling as depicted in Figure 7. Importantly, CP-AMPAR signaling is then required, along with NMDAR signaling, to rapidly trigger AKAP-CaN mediated removal of the newly recruited GluA2-lacking CP-AMPARs, along with GluA2-containing receptors, to allow for optimal LTD expression. If CP-AMPAR signaling is not engaged, such as in 150ΔPKA mice or with continuous application of NASPM, then LTD expression is substantially reduced but not eliminated. Thus, NMDAR signaling alone is capable of removing GluA2-containing AMPARs to induce some LTD, but additional contributions from CP-AMPARs are required for robust LTD expression. Figure 7 depicts two distinct, sequential stages: 1) NMDAR and PKA-dependent CP-AMPAR recruitment and 2) NMDAR, CP-AMPAR and CaN-dependent AMPAR removal, accompanied by spine shrinkage (Zhou et al., 2004) and disruption of AKAP150 membrane targeting and PSD-95 interactions that may prevent AMPARs from returning to the synapse (Smith et al., 2006), but in reality these processes must be occurring almost simultaneously and continuously during the LTD induction stimulus to prevent potentiation and promote depression.

Previous studies found that pharmacological inhibition of PKA activity or AKAP-PKA anchoring can lead to depression of both synaptic and extrasynaptic AMPAR activity that occludes subsequent LTD induction (Kameyama et al., 1998; Rosenmund et al., 1994; Snyder et al., 2005; Tavalin et al., 2002). However, even acute inhibition of PKA activity that does not result in depression of basal AMPAR transmission can inhibit LTD (Lu et al., 2008). In addition, LTD is impaired in AKAP150 knock-out and PKA-anchoring deficient D36 knock-in mice, yet both strains exhibit no decreases in basal AMPAR transmission and at best partial decreases in basal GluA1 S845 phosphorylation (Lu et al., 2007; Lu et al., 2008; Tunquist et al., 2008; Zhang et al., 2013). Likewise, here in 150ΔPKA mice we found impaired LTD but only a ~40% reduction in basal S845 phosphorylation and no decrease in basal AMPAR transmission. Thus, while prior inhibition of AKAP-PKA signaling can lead to depression that occludes LTD, AKAP-PKA signaling also plays a more dynamic role during LTD induction, which we now show involves the transient recruitment of CP-AMPAR to synapses, a mechanism previously only implicated in AKAP-PKA LTP regulation (Lu et al., 2007).

A requirement for active PKA signaling during LTD induction was proposed in studies characterizing AKAP150 D36mice (Lu et al., 2008), but linking impaired LTD in D36 mice to PKA signaling deficits was complicated by subsequent work showing substantial increases in the number of dendritic spines and overall basal excitatory and inhibitory input to CA1 neurons in juvenile D36 mice (Lu et al., 2011). Importantly, we only observed a very small increase in spine density and did not detect any significant changes in excitatory or inhibitory input to CA1 neurons in 150ΔPKA mice. The reasons for these differences in basal transmission measurements are unclear but could be due to the ΔPKA deletion being

more specific than the larger D36 truncation, as well as possibly differences in recording conditions. Nonetheless, the findings of impaired LTD in both 150ΔPKA and D36 mice are in agreement and indicate that changes in basal transmission in D36 mice had little impact on the impaired LTD phenotype.

Our findings and model are also consistent with the idea that highly dynamic, localized cycles of phosphorylation and dephosphorylation confined to a small pool of GluA1 homomers can have major impacts on synaptic function (Guire et al., 2008). As mentioned above, localized, rapid phosphorylation cycling would be impossible to detect using biochemical methods, thus the absolute amounts and steady-state levels of bulk GluA1 phosphorylation are not likely to fully represent underlying signaling dynamics. Nonetheless, biochemical measurements showing S845 phosphorylation decreases in 150ΔPKA and increases in 150ΔPIX mice may still reflect that imbalances in local, postsynaptic PKA versus CaN signaling are also occurring in real-time. It will be interesting to determine whether other kinases that phosphorylate GluA1, such as CaMKII which is required for both LTP and LTD (Coultrap et al., 2014), also regulate CP-AMPAR synaptic recruitment and/or removal in coordination with PKA and CaN during LTD.

The model in Figure 7 depicts the CP-AMPARs participating in LTD induction as being physically recruited to synapse, but alternatively these CP-AMPARs could be functionally recruited to participate in synaptic signaling from peri-synaptic locations due to glutamate spill over during prolonged LFS. Such an engagement of peri-synaptic CP-AMPARs could be consistent with work by He et al. showing that glutamate spill-over can unmask an antagonist-sensitive pool of CP-AMPARs that is removed by LTD induction in WT mice and is not present in S845A mice (He et al., 2009). Our experiments continuously applying NASPM during LFS cannot distinguish between these two possibilities because both the stimulus and the antagonist were presented together for a long period of time such that there is no way to tell when and where use-dependent CP-AMPAR block occurs. However, the findings of more pronounced LTD inhibition, and even potentiation, when NASPM is washed out post-induction suggest that CP-AMPARs are physically recruited and then retained in the synapse if blocked by NASPM to prevent removal. In addition, our measurements of NASPM-sensitive AMPAR rectification during LTD induction, which we performed while pausing LFS delivery (thus spill-over unlikely), are also consistent with transient physical CP-AMPAR recruitment to the synapse. Accordingly, in 150ΔPIX mice, where CP-AMPARs are not removed after induction (as shown by antagonist sensitivity and rectification), LTD expression is obscured by the continuing presence of these higher-conductance receptors.

Although secondary to our main findings of CP-AMPAR engagement in LTD, we also made interesting new observations regarding the CP-AMPAR dependence of LTP that reinforce the idea that there is a remarkable amount of developmental plasticity in LTP mechanisms. Our findings of a transition in the CP-AMPAR antagonist sensitivity of LTP between P14 and P17 are in agreement with a previous study that found changes in the CP-AMPAR dependence of LTP induced by 1×100 Hz HFS during the third postnatal week (Lu et al., 2007). However, our results here indicate that this developmental switch away from LTP engagement of CP-AMPARs is more abrupt than previously appreciated and occurs over

only ~3 days. Although differences in LTP induction stimuli and recording conditions can also be relevant (Gray et al., 2007; Guire et al., 2008; Lu et al., 2007), such an abrupt developmental transition could explain how different studies that analyzed 2–3 week-old animals obtained opposite results regarding CP-AMPARs in LTP, depending on whether the age distribution was possibly skewed toward 2 or 3 weeks (Adesnik and Nicoll, 2007; Gray et al., 2007; Plant et al., 2006; Yang et al., 2010). Indeed, in our prior work showing that CP-AMPARs contribute to enhanced LTP in 150ΔPIX mice, we recorded from a mix of 2–3 week-old mice and found, using 1×100 Hz induction as here, that CA1 LTP in WT mice was not inhibited by IEM1460 (Sanderson et al., 2012).

Our present result that ≤2 week-old 150ΔPKA mice express normal LTP that does not depend on CP-AMPARs also supports the collective findings of previous work showing that LTP mechanisms are remarkably adaptable in juvenile animals compared to adults. In particular, GluA1 knock-out, S845A/S831A, and AKAP150 D36 mice all exhibit impaired LTP as adults but express normal LTP as juveniles (Jensen et al., 2003; Lee et al., 2003; Lu et al., 2007; Zamanillo et al., 1999). Accordingly, elegant work by Granger et al. demonstrated that either GluA1 or GluA2 alone (or even a kainate receptor) can support LTP at CA1 synapses in ~2–3 week-old animals, providing that a sufficient extrasynaptic reserve pool of receptors exists (Granger et al., 2013). Thus, as proposed by Granger et al., LTP in juveniles may be more dependent on and driven by PSD structural remodeling to create more slots for AMPARs, but these slots then have the potential to be filled by a variety of different receptor types through the anchoring functions of auxiliary subunits, such as Transmembrane AMPA Receptor Regulatory Proteins (TARPs), and through regulation by a variety of overlapping signaling mechanisms (Tomita et al., 2005). Yet, by adulthood, the extrasynaptic AMPAR reserve pool and LTP become much more dependent on GluA1, and in parallel the importance of AKAP-PKA signaling, GluA1 phosphorylation, and CP-AMPARs in regulating LTP increase. Overall, adaptability in LTP and its underlying mechanisms appears to be a characteristic of the juvenile hippocampus that decreases by adulthood. However, as shown here, some of the same molecules and mechanisms that are non-essential for LTP in juveniles can at the same time still be crucial for LTD. While the prominence of NMDAR-dependent LTD decreases during postnatal development to adulthood, NMDAR-LTD mechanisms, including GluA1 S845 regulation, appear to remain more constant during development (Babiec et al., 2014; Dudek and Bear, 1993; He et al., 2009; Lee et al., 2003; Lee et al., 2010). Importantly, He et al. demonstrated that LTD removes peri-synaptic CP-AMPARs in an S845-dependent manner in 3–4 week-old mice. However, it remains to be determined whether CP-AMPAR contributions to LTD remain constant on through to adulthood.

In addition to having over-sized contributions to synaptic strength due to high single-channel conductance, synaptic CP-AMPARs can also confer other unique properties resulting in plasticity of plasticity itself, so-called meta-plasticity. Meta-plastic changes conferred by CP-AMPARs include enhanced LTP at hippocampal synapses (Megill et al., 2015; Sanderson et al., 2012) and the ability to express a unique mGluR1-mediated mechanism that removes CP-AMPARs from synapses in the amygdala, nucleus accumbens, ventral tegmentum, and cerebellum (Bellone et al., 2011; Clem and Huganir, 2013; Kelly et al., 2009; Loweth et al., 2013). Here we show that CP-AMPAR recruitment to synapses can also

positively regulate NMDAR-dependent LTD, but only if CP-AMPARs remain in the synapse transiently, such that the change in meta-plasticity is brief. If the precise balance of PKA/CaN signaling shifts in either direction, then meta-plasticity is disrupted and LTD is impaired either due to insufficient CP-AMPAR recruitment or removal. Importantly, only through co-anchoring of PKA and CaN to AKAP150 can such precisely-balanced bi-directional control be achieved to produce a transient burst in CP-AMPAR Ca^{2+} signaling that augments NMDAR signaling in LTD.

EXPERIMENTAL PROCEDURES

Animal use and care

All animal procedures were approved by the University of Colorado-Denver Institutional Animal Care and Use Committee in accordance with National Institutes of Health-United States Public Health Service guidelines. Production of AKAP150 ΔPIX mice and ΔPKA mice was previously described in Sanderson et al., 2012 and Murphy et al., 2014, respectively. Both mouse alleles (AKAP150ΔPKA, RRID: MGI_5635498; AKAP150ΔPIX, RRID: MGI_5448682) were backcrossed to C57Bl6J several generations but then maintained, along with related WT controls, on a mixed C57Bl6J(~75%)/129X1/SvJ(~25%) background. Both male and female between 11 and 21 days of age were used.

Subcellular fractionation and immunoblotting of hippocampal tissue and dendritic spine analysis by Golgi staining

Subcellular fractionation, immunoblotting, and Golgi staining to visualize dendritic spines were performed essentially as previously described (Sanderson et al., 2012). More detailed experimental information is provided in the on-line Supplemental Material.

Electrophysiology

CA1 fEPSP recordings and whole-cell EPSC and IPSC recordings were carried out using acute hippocampal slices essentially as described in our previous work (Sanderson et al., 2012). More detailed experimental information is provided in the on-line Supplemental Material.

Statistical analysis

LTP and LTD time-course data were analyzed using two-way ANOVA in Prism (GraphPad). Significance is reported as $p<0.05$ and data are expressed as mean ± SEM. Group comparisons where indicated were performed in Prism using one-way ANOVA with Dunnett's (for multiple comparisons to control) or Newman-Keuls (for multiple comparisons between conditions) post-hoc analysis. For one-way ANOVA, only $p>0.05$ (not significant, ns), $*p<0.05$, $**p<0.01$, or $***p<0.001$ are provided by the software. Pair-wise comparisons or comparisons of normalized data to set values (i.e. 0.0, 1.0 or 100) were performed in Prism using Student's t-test or one-sample t-test, respectively. For t-tests and two-way ANOVA actual p values are provided except when $p<0.0001$.

Supplementary Material

Refer to Web version on PubMed Central for supplementary material.

Acknowledgments

We thank Emily Gibson and Philip Lam for technical support. We thank Drs. Timothy Benke, Matthew Kennedy, and K. Ulrich Bayer for critical reading of the manuscript. This work was supported by NIH grant R01NS040701 to MLD. Contents are the authors' sole responsibility and do not necessarily represent official NIH views.

References

Adesnik H, Nicoll RA. Conservation of glutamate receptor 2-containing AMPA receptors during long-term potentiation. J Neurosci. 2007; 27:4598–4602. [PubMed: 17460072]

Babiec WE, Guglietta R, Jami SA, Morishita W, Malenka RC, O'Dell TJ. Ionotropic NMDA Receptor Signaling Is Required for the Induction of Long-Term Depression in the Mouse Hippocampal CA1 Region. J Neurosci. 2014; 34:5285–5290. [PubMed: 24719106]

Beattie EC, Carroll RC, Yu X, Morishita W, Yasuda H, von Zastrow M, Malenka RC. Regulation of AMPA receptor endocytosis by a signaling mechanism shared with LTD. Nat Neurosci. 2000; 3:1291–1300. [PubMed: 11100150]

Bellone C, Mameli M, Luscher C. In utero exposure to cocaine delays postnatal synaptic maturation of glutamatergic transmission in the VTA. Nat Neurosci. 2011; 14:1439–1446. [PubMed: 21964489]

Clem RL, Huganir RL. Calcium-permeable AMPA receptor dynamics mediate fear memory erasure. Science. 2010; 330:1108–1112. [PubMed: 21030604]

Clem RL, Huganir RL. Norepinephrine enhances a discrete form of long-term depression during fear memory storage. J Neurosci. 2013; 33:11825–11832. [PubMed: 23864672]

Collingridge GL, Peineau S, Howland JG, Wang YT. Long-term depression in the CNS. Nat Rev Neurosci. 2010; 11:459–473. [PubMed: 20559335]

Coultrap SJ, Freund RK, O'Leary H, Sanderson JL, Roche KW, Dell'Acqua ML, Bayer KU. Autonomous CaMKII mediates both LTP and LTD using a mechanism for differential substrate site selection. Cell Rep. 2014; 6:431–437. [PubMed: 24485660]

Diering GH, Gustina AS, Huganir RL. PKA-GluA1 coupling via AKAP5 controls AMPA receptor phosphorylation and cell-surface targeting during bidirectional homeostatic plasticity. Neuron. 2014; 84:790–805. [PubMed: 25451194]

Dudek SM, Bear MF. Homosynaptic long-term depression in area CA1 of hippocampus and effects of N-methyl-D-aspartate receptor blockade. Proc Natl Acad Sci U S A. 1992; 89:4363–4367. [PubMed: 1350090]

Dudek SM, Bear MF. Bidirectional long-term modification of synaptic effectiveness in the adult and immature hippocampus. J Neurosci. 1993; 13:2910–2918. [PubMed: 8331379]

Ehlers MD. Reinsertion or degradation of AMPA receptors determined by activity-dependent endocytic sorting. Neuron. 2000; 28:511–525. [PubMed: 11144360]

Esteban JA, Shi SH, Wilson C, Nuriya M, Huganir RL, Malinow R. PKA phosphorylation of AMPA receptor subunits controls synaptic trafficking underlying plasticity. Nat Neurosci. 2003; 6:136–143. [PubMed: 12536214]

Goel A, Xu LW, Snyder KP, Song L, Goenaga-Vazquez Y, Megill A, Takamiya K, Huganir RL, Lee HK. Phosphorylation of AMPA receptors is required for sensory deprivation-induced homeostatic synaptic plasticity. PLoS One. 2011; 6:e18264. [PubMed: 21483826]

Granger AJ, Shi Y, Lu W, Cerpas M, Nicoll RA. LTP requires a reserve pool of glutamate receptors independent of subunit type. Nature. 2013; 493:495–500. [PubMed: 23235828]

Gray EE, Fink AE, Sarinana J, Vissel B, O'Dell TJ. Long-term potentiation in the hippocampal CA1 region does not require insertion and activation of GluR2-lacking AMPA receptors. J Neurophysiol. 2007; 98:2488–2492. [PubMed: 17652419]

Guire ES, Oh MC, Soderling TR, Derkach VA. Recruitment of calcium-permeable AMPA receptors during synaptic potentiation is regulated by CaM-kinase I. J Neurosci. 2008; 28:6000–6009. [PubMed: 18524905]

He K, Song L, Cummings LW, Goldman J, Huganir RL, Lee HK. Stabilization of Ca2+-permeable AMPA receptors at perisynaptic sites by GluR1-S845 phosphorylation. Proc Natl Acad Sci U S A. 2009; 106:20033–20038. [PubMed: 19892736]

Hosokawa T, Mitsushima D, Kaneko R, Hayashi Y. Stoichiometry and phosphoisotypes of hippocampal AMPA-type glutamate receptor phosphorylation. Neuron. 2015; 85:60–67. [PubMed: 25533481]

Hu H, Real E, Takamiya K, Kang MG, Ledoux J, Huganir RL, Malinow R. Emotion enhances learning via norepinephrine regulation of AMPA-receptor trafficking. Cell. 2007; 131:160–173. [PubMed: 17923095]

Huganir RL, Nicoll RA. AMPARs and Synaptic Plasticity: The Last 25 Years. Neuron. 2013; 80:704–717. [PubMed: 24183021]

Jensen V, Kaiser KM, Borchardt T, Adelmann G, Rozov A, Burnashev N, Brix C, Frotscher M, Andersen P, Hvalby O, et al. A juvenile form of postsynaptic hippocampal long-term potentiation in mice deficient for the AMPA receptor subunit GluR-A. J Physiol. 2003; 553:843–856. [PubMed: 14555717]

Jurado S, Biou V, Malenka RC. A calcineurin/AKAP complex is required for NMDA receptor-dependent long-term depression. Nat Neurosci. 2010; 13:1053–1055. [PubMed: 20694001]

Kameyama K, Lee HK, Bear MF, Huganir RL. Involvement of a postsynaptic protein kinase A substrate in the expression of homosynaptic long-term depression. Neuron. 1998; 21:1163–1175. [PubMed: 9856471]

Kelly L, Farrant M, Cull-Candy SG. Synaptic mGluR activation drives plasticity of calcium-permeable AMPA receptors. Nat Neurosci. 2009; 12:593–601. [PubMed: 19377472]

Kim S, Ziff EB. Calcineurin mediates synaptic scaling via synaptic trafficking of Ca2+-permeable AMPA receptors. PLoS Biol. 2014; 12:e1001900. [PubMed: 24983627]

Lee HK, Barbarosie M, Kameyama K, Bear MF, Huganir RL. Regulation of distinct AMPA receptor phosphorylation sites during bidirectional synaptic plasticity. Nature. 2000; 405:955–959. [PubMed: 10879537]

Lee HK, Kameyama K, Huganir RL, Bear MF. NMDA induces long-term synaptic depression and dephosphorylation of the GluR1 subunit of AMPA receptors in hippocampus. Neuron. 1998; 21:1151–1162. [PubMed: 9856470]

Lee HK, Takamiya K, Han JS, Man H, Kim CH, Rumbaugh G, Yu S, Ding L, He C, Petralia RS, et al. Phosphorylation of the AMPA receptor GluR1 subunit is required for synaptic plasticity and retention of spatial memory. Cell. 2003; 112:631–643. [PubMed: 12628184]

Lee HK, Takamiya K, He K, Song L, Huganir RL. Specific roles of AMPA receptor subunit GluR1 (GluA1) phosphorylation sites in regulating synaptic plasticity in the CA1 region of hippocampus. J Neurophysiol. 2010; 103:479–489. [PubMed: 19906877]

Liu SJ, Zukin RS. Ca2+-permeable AMPA receptors in synaptic plasticity and neuronal death. Trends Neurosci. 2007; 30:126–134. [PubMed: 17275103]

Loweth JA, Scheyer AF, Milovanovic M, Lacrosse AL, Flores-Barrera E, Werner CT, Li X, Ford KA, Le T, Olive MF, et al. Synaptic depression via mGluR1 positive allosteric modulation suppresses cue-induced cocaine craving. Nat Neurosci. 2013

Lu W, Shi Y, Jackson AC, Bjorgan K, During MJ, Sprengel R, Seeburg PH, Nicoll RA. Subunit composition of synaptic AMPA receptors revealed by a single-cell genetic approach. Neuron. 2009; 62:254–268. [PubMed: 19409270]

Lu Y, Allen M, Halt AR, Weisenhaus M, Dallapiazza RF, Hall DD, Usachev YM, McKnight GS, Hell JW. Age-dependent requirement of AKAP150-anchored PKA and GluR2-lacking AMPA receptors in LTP. EMBO J. 2007; 26:4879–4890. [PubMed: 17972919]

Lu Y, Zha XM, Kim EY, Schachtele S, Dailey ME, Hall DD, Strack S, Green SH, Hoffman DA, Hell JW. A kinase anchor protein 150 (AKAP150)-associated protein kinase A limits dendritic spine density. J Biol Chem. 2011; 286:26496–26506. [PubMed: 21652711]

Lu Y, Zhang M, Lim IA, Hall DD, Allen M, Medvedeva Y, McKnight GS, Usachev YM, Hell JW. AKAP150-anchored PKA activity is important for LTD during its induction phase. J Physiol. 2008; 586:4155–4164. [PubMed: 18617570]

Man HY, Sekine-Aizawa Y, Huganir RL. Regulation of {alpha}-amino-3-hydroxy-5-methyl-4-isoxazolepropionic acid receptor trafficking through PKA phosphorylation of the Glu receptor 1 subunit. Proc Natl Acad Sci U S A. 2007; 104:3579–3584. [PubMed: 17360685]

McCutcheon JE, Wang X, Tseng KY, Wolf ME, Marinelli M. Calcium-permeable AMPA receptors are present in nucleus accumbens synapses after prolonged withdrawal from cocaine self-administration but not experimenter-administered cocaine. J Neurosci. 2011; 31:5737–5743. [PubMed: 21490215]

Megill A, Tran T, Eldred K, Lee NJ, Wong PC, Hoe HS, Kirkwood A, Lee HK. Defective Age-Dependent Metaplasticity in a Mouse Model of Alzheimer's Disease. J Neurosci. 2015; 35:11346–11357. [PubMed: 26269641]

Mulkey RM, Endo S, Shenolikar S, Malenka RC. Involvement of a calcineurin/inhibitor-1 phosphatase cascade in hippocampal long-term depression. Nature. 1994; 369:486–488. [PubMed: 7515479]

Mulkey RM, Malenka RC. Mechanisms underlying induction of homosynaptic long-term depression in area CA1 of the hippocampus. Neuron. 1992; 9:967–975. [PubMed: 1419003]

Murphy JG, Sanderson JL, Gorski JA, Scott JD, Catterall WA, Sather WA, Dell'Acqua ML. AKAP-anchored PKA maintains neuronal L-type calcium channel activity and NFAT transcriptional signaling. Cell Rep. 2014; 7:1577–1588. [PubMed: 24835999]

Nabavi S, Kessels HW, Alfonso S, Aow J, Fox R, Malinow R. Metabotropic NMDA receptor function is required for NMDA receptor-dependent long-term depression. Proc Natl Acad Sci U S A. 2013; 110:4027–4032. [PubMed: 23431133]

Oh MC, Derkach VA, Guire ES, Soderling TR. Extrasynaptic membrane trafficking regulated by GluR1 serine 845 phosphorylation primes AMPA receptors for long-term potentiation. J Biol Chem. 2006; 281:752–758. [PubMed: 16272153]

Oliveria SF, Dell'Acqua ML, Sather WA. AKAP79/150 anchoring of calcineurin controls neuronal L-type Ca2+ channel activity and nuclear signaling. Neuron. 2007; 55:261–275. [PubMed: 17640527]

Plant K, Pelkey KA, Bortolotto ZA, Morita D, Terashima A, McBain CJ, Collingridge GL, Isaac JT. Transient incorporation of native GluR2-lacking AMPA receptors during hippocampal long-term potentiation. Nat Neurosci. 2006; 9:602–604. [PubMed: 16582904]

Qian H, Matt L, Zhang M, Nguyen M, Patriarchi T, Koval OM, Anderson ME, He K, Lee HK, Hell JW. beta2-Adrenergic receptor supports prolonged theta tetanus-induced LTP. J Neurophysiol. 2012; 107:2703–2712. [PubMed: 22338020]

Raymond CR, Ireland DR, Abraham WC. NMDA receptor regulation by amyloid-beta does not account for its inhibition of LTP in rat hippocampus. Brain Res. 2003; 968:263–272. [PubMed: 12663096]

Rosenmund C, Carr DW, Bergeson SE, Nilaver G, Scott JD, Westbrook GL. Anchoring of protein kinase A is required for modulation of AMPA/kainate receptors on hippocampal neurons. Nature. 1994; 368:853–856. [PubMed: 8159245]

Rozov A, Sprengel R, Seeburg PH. GluA2-lacking AMPA receptors in hippocampal CA1 cell synapses: evidence from gene-targeted mice. Front Mol Neurosci. 2012; 5:22. [PubMed: 22375105]

Rozov A, Zilberter Y, Wollmuth LP, Burnashev N. Facilitation of currents through rat Ca2+-permeable AMPA receptor channels by activity-dependent relief from polyamine block. J Physiol. 1998; 511(Pt 2):361–377. [PubMed: 9706016]

Sanderson JL, Gorski JA, Gibson ES, Lam P, Freund RK, Chick WS, Dell'Acqua ML. AKAP150-anchored calcineurin regulates synaptic plasticity by limiting synaptic incorporation of Ca2+-permeable AMPA receptors. J Neurosci. 2012; 32:15036–15052. [PubMed: 23100425]

Smith KE, Gibson ES, Dell'Acqua ML. cAMP-dependent protein kinase postsynaptic localization regulated by NMDA receptor activation through translocation of an A-kinase anchoring protein scaffold protein. J Neurosci. 2006; 26:2391–2402. [PubMed: 16510716]

Snyder EM, Colledge M, Crozier RA, Chen WS, Scott JD, Bear MF. Role for A kinase-anchoring proteins (AKAPS) in glutamate receptor trafficking and long term synaptic depression. J Biol Chem. 2005; 280:16962–16968. [PubMed: 15718245]

Soares C, Lee KF, Nassrallah W, Beique JC. Differential subcellular targeting of glutamate receptor subtypes during homeostatic synaptic plasticity. J Neurosci. 2013; 33:13547–13559. [PubMed: 23946413]

Stubblefield EA, Benke TA. Distinct AMPA-type glutamatergic synapses in developing rat CA1 hippocampus. J Neurophysiol. 2010; 104:1899–1912. [PubMed: 20685930]

Sun X, Zhao Y, Wolf ME. Dopamine receptor stimulation modulates AMPA receptor synaptic insertion in prefrontal cortex neurons. J Neurosci. 2005; 25:7342–7351. [PubMed: 16093384]

Sutton MA, Ito HT, Cressy P, Kempf C, Woo JC, Schuman EM. Miniature neurotransmission stabilizes synaptic function via tonic suppression of local dendritic protein synthesis. Cell. 2006; 125:785–799. [PubMed: 16713568]

Tavalin SJ, Colledge M, Hell JW, Langeberg LK, Huganir RL, Scott JD. Regulation of GluR1 by the A-kinase anchoring protein 79 (AKAP79) signaling complex shares properties with long-term depression. J Neurosci. 2002; 22:3044–3051. [PubMed: 11943807]

Thiagarajan TC, Lindskog M, Tsien RW. Adaptation to synaptic inactivity in hippocampal neurons. Neuron. 2005; 47:725–737. [PubMed: 16129401]

Tomita S, Stein V, Stocker TJ, Nicoll RA, Bredt DS. Bidirectional synaptic plasticity regulated by phosphorylation of stargazin-like TARPs. Neuron. 2005; 45:269–277. [PubMed: 15664178]

Tunquist BJ, Hoshi N, Guire ES, Zhang F, Mullendorff K, Langeberg LK, Raber J, Scott JD. Loss of AKAP150 perturbs distinct neuronal processes in mice. Proc Natl Acad Sci U S A. 2008; 105:12557–12562. [PubMed: 18711127]

Weisenhaus M, Allen ML, Yang L, Lu Y, Nichols CB, Su T, Hell JW, McKnight GS. Mutations in AKAP5 disrupt dendritic signaling complexes and lead to electrophysiological and behavioral phenotypes in mice. PLoS One. 2010; 5:e10325. [PubMed: 20428246]

Woolfrey KM, Dell'Acqua ML. Coordination of Protein Phosphorylation and Dephosphorylation in Synaptic Plasticity. J Biol Chem. 2015; 290:28604–28612. [PubMed: 26453308]

Yang Y, Wang XB, Frerking M, Zhou Q. Delivery of AMPA receptors to perisynaptic sites precedes the full expression of long-term potentiation. Proc Natl Acad Sci U S A. 2008; 105:11388–11393. [PubMed: 18682558]

Yang Y, Wang XB, Zhou Q. Perisynaptic GluR2-lacking AMPA receptors control the reversibility of synaptic and spines modifications. Proc Natl Acad Sci U S A. 2010; 107:11999–12004. [PubMed: 20547835]

Zamanillo D, Sprengel R, Hvalby O, Jensen V, Burnashev N, Rozov A, Kaiser KM, Koster HJ, Borchardt T, Worley P, et al. Importance of AMPA receptors for hippocampal synaptic plasticity but not for spatial learning. Science. 1999; 284:1805–1811. [PubMed: 10364547]

Zhang M, Patriarchi T, Stein IS, Qian H, Matt L, Nguyen M, Xiang YK, Hell JW. Adenylyl cyclase anchoring by a kinase anchor protein AKAP5 (AKAP79/150) is important for postsynaptic beta-adrenergic signaling. J Biol Chem. 2013; 288:17918–17931. [PubMed: 23649627]

Zhou Q, Homma KJ, Poo MM. Shrinkage of dendritic spines associated with long-term depression of hippocampal synapses. Neuron. 2004; 44:749–757. [PubMed: 15572107]

Highlights

- AKAP150-PKA promotes GluA1 phosphorylation and CP-AMPAR synaptic recruitment in LTP
- AKAP150-PKA signaling also recruits CP-AMPARs to synapses during LTD induction
- AKAP150-Calcineurin signaling rapidly removes CP-AMPARs recruited during LTD
- CP-AMPAR recruitment confers a transient meta-plastic state that promotes LTD

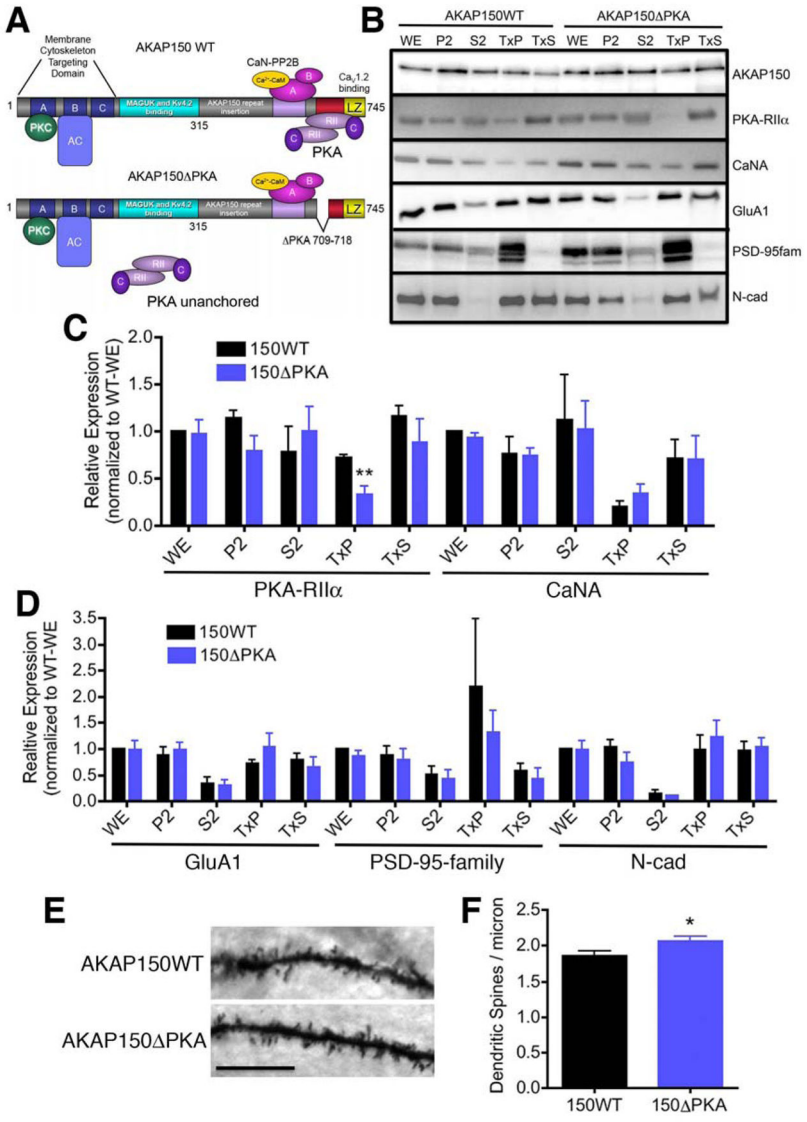

Figure 1. PKA-anchoring deficient AKAP150Δ PKA mice have reduced PKA-RII levels in hippocampal PSD fractions

(A) Diagram of AKAP150 primary structure showing the location of functional domains and binding sites for the indicated proteins. AC=adenylyl cyclase. Location of the ΔPKA (Δ709–718) deletion that disrupts PKA anchoring is indicated. Note: The primary sequence and MW of mouse AKAP150 differs from human AKAP79 due to the insertion into the *Akap5* gene of a repetitive sequence found only in rodents that has no known function.

(B) Subcellular fractionation and immunoblotting of hippocampal tissue from WT and ΔPKA mice showing expression patterns for the indicated proteins in the AKAP150 signaling complex. WE = whole extract, P2 = synaptosomes, S2 = cytosol + light membranes, TxP = crude PSD/Triton-insoluble fraction of P2, TxS = Triton-soluble fraction of P2.

(C) Quantification of PKA-RIIα and CaNA expression levels in subcellular fractions from panel B normalized to WE for WT, **p<0.01 unpaired t-test.

(D) Quantification of expression of additional AKAP150 binding partners (GluA1, PSD-95 family MAGUK scaffolds, N-cadherin) for subcellular fractions in panel B normalized to WE for WT.

(E) Images of Golgi-stained dendrites in CA1 stratum radiatum of AKAP150 WT and ΔPKA mice.

(F) Quantification of dendritic spine numbers per μm in Golgi-stained dendrites as in panel E.

In all graphs data are mean ± SEM.

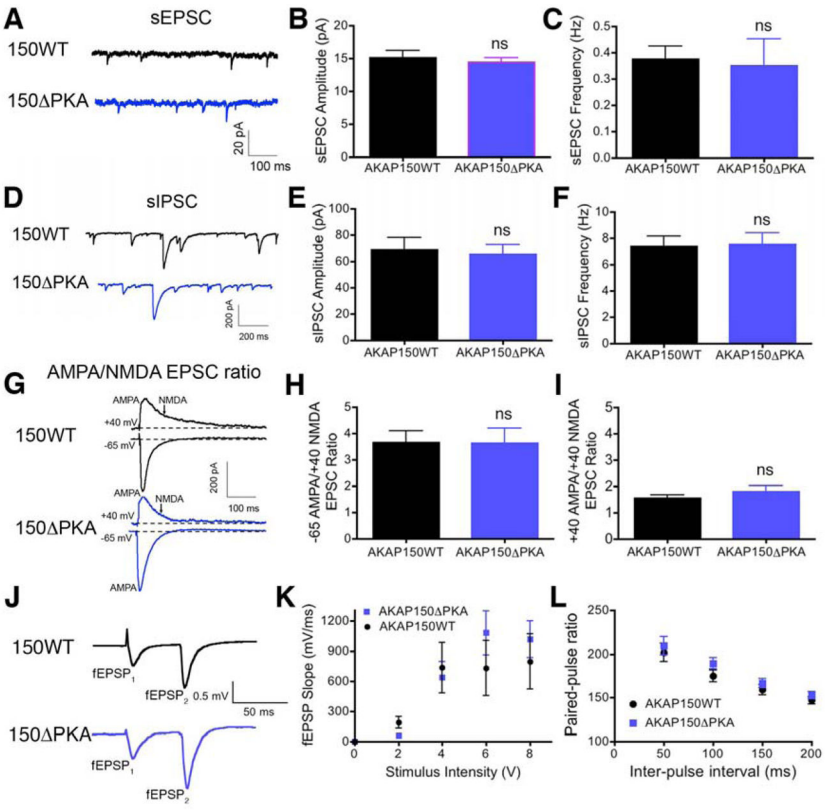

Figure 2. Basal excitatory and inhibitory synaptic transmission is normal in CA1 pyramidal neurons of AKAP150Δ PKA mice

(A) Representative current records and **(B)** graphs of mean sEPSC amplitude (pA) and **(C)** frequency (Hz).

(D) Representative current records and **(E)** graphs of mean sIPSC amplitude and **(F)** frequency. See also Figure S1.

(G) Representative current records of evoked inward AMPA (−65 mV holding potential) and outward AMPA and NMDA EPSCs (+40 mV holding potential).

(H) Graphs of mean −65AMPA/+40NMDA and **(I)** +40AMPA/+NMDA EPSC current ratios.

(J) Representative fEPSP recordings from area CA1 stratum radiatum shown from PPR experiments in panel L using an inter-stimulus interval of 50 ms.

(K) Input/output plots of CA1 fEPSP slope (mV/ms) evoked in response to increasing intensity of presynaptic SC stimulation (V).

(L) Plots of CA1 paired-pulse ratios (PPR = $fEPSP_2$ amplitude/$fEPSP_1$ amplitude) in response to paired-pulse SC stimulation using a range of inter-stimulus intervals.

In all graphs data are mean ± SEM.

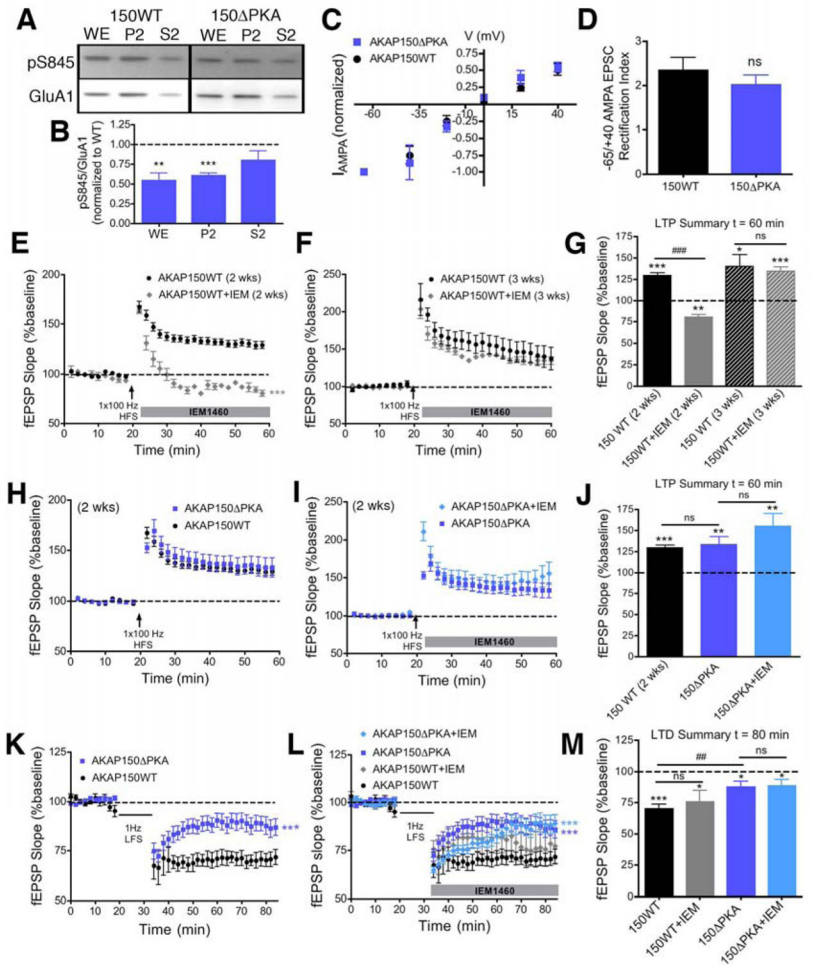

Figure 3. AKAP150Δ PKA mice exhibit reduced GluA1 S845 phosphorylation, loss of CP-AMPAR recruitment during LTP, and impaired LTD at SC-CA1 synapses

(A) Representative immunoblots of hippocampal WE (whole extract), P2 (synaptosomes), and S2 (cytosol + light membranes) fractions mice using anti-pS845 (upper panel) followed by stripping and re-probing with anti-GluA1 (lower panel).

(B) Quantification of pS845/total GluA1 immunoreactivity normalized to WT controls show reductions in S845 phosphorylation for 150ΔPKA mice in WE and P2 fractions. **p<0.01, ***p<0.001 one-sample t-test to WT (normalized = 1.0).

(**C**) Normalized I/V plots for evoked AMPA EPSCs (values plotted on the y-axis are normalized to the −65 mV mean value for that genotype) and (**D**) Graph of −65 mV/+40 mV EPSC rectification indices reveal no changes in basal AMPAR subunit composition at SC-CA1 synapses of AKAP150 ΔPKA compared to WT mice.

(**E**) Plots of fEPSP (normalized to % of baseline) over time showing that LTP expression at SC-CA1 synapses is inhibited by addition of the CP-AMPAR antagonist IEM1460 (70 μM; gray bar) after HFS induction (1×100Hz, 1s) in ≤ 2 week-old (t=50–56 min ***p<0.0001 two-way ANOVA to WT control) but not (**F**) ~3 week-old WT mice.

(**G**) Summary graph for LTP expression (%baseline) at t=60 min for experiments in panels E and F. *p<0.05, **p<0.01, **p<0.001 to respective pre-LTP values; ###p<0.001 to WT t=60 min; ns p>0.05; unpaired t-tests.

(**H**) ≤ 2 week-old 150ΔPKA mice LTP expression is normal compared to WT but (**I**) is insensitive to the CP-AMPAR antagonist IEM1460 (70 μM; gray bar).

(**J**) Summary graph for LTP expression (%baseline) at t=60 min for experiments in panels H and I. **p<0.01, **p<0.001 to respective pre-LTP values; ns p>0.05; unpaired t-tests.

(**K**) ≤ 2 week-old 150ΔPKA mice LTD expression induced by LFS (1 Hz, 15 min) is reduced compared to WT (t=70–80 min ***p<0.0001 two-way ANOVA to WT).

(**L**) Addition of the CP-AMPAR antagonist IEM1460 (70 μM; gray bar) after LFS induction does not impact the level of LTD expression in either WT or 150ΔPKA mice.

(**M**) Summary graph for LTD expression (%baseline) at t=80 min for experiments in panels K and L. *p<0.05, **p<0.01 to respective pre-LTP values; ##p<0.01 to WT t=80 min; unpaired t-tests.

In all graphs data are mean ± SEM.

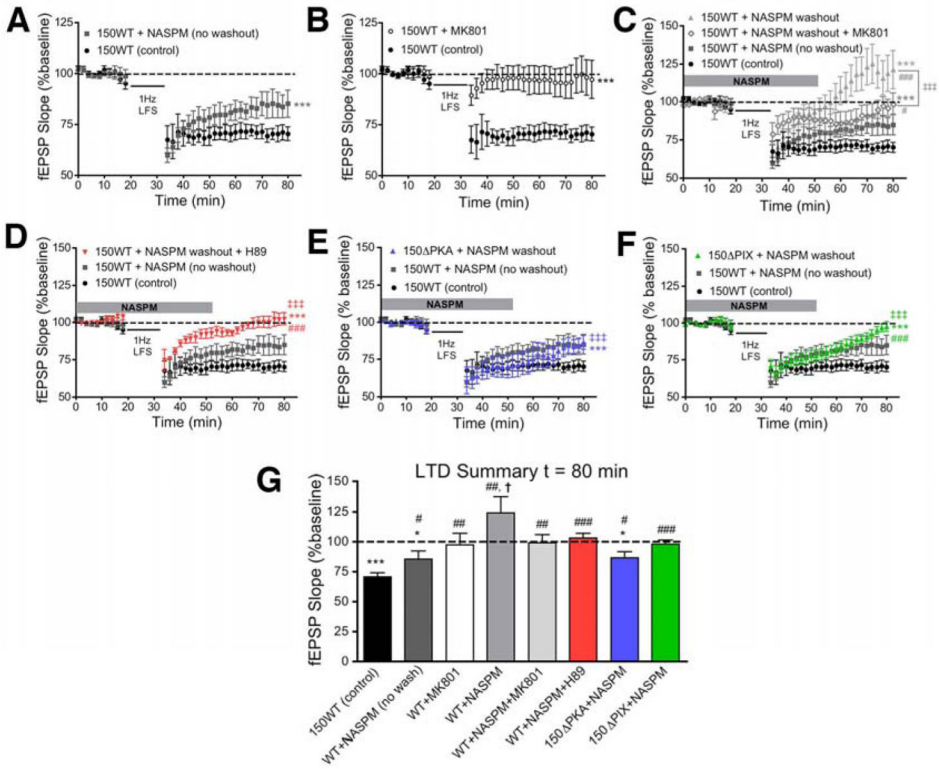

Figure 4. Antagonist application during induction reveals novel roles for CP-AMPAR and AKAP150-PKA signaling in NMDAR-dependent LTD at SC-CA1 synapses

(A) Continuous application of CP-AMPAR antagonist NASPM (20 μM; no washout) reduces LTD expression in ≤ 2 week-old WT mice (t=70–80 min ***p<0.0001 two-way ANOVA to WT control). See also Figure S2.

(B) Continuous application of NMDAR antagonist MK801 (10 μM; no washout) blocks LTD induction in ≤ 2 week-old WT mice (***p<0.0001 two-way ANOVA to WT control).

(C) NASPM washout after LTD induction (gray bar indicates the estimated time of washout) inhibits LTD expression and results in variable synaptic potentiation that is prevented by MK801 co-application (t=70–80 min ***p<0.0001 to WT control; $^{\#}$p<0.05, $^{\#\#\#}$p<0.0001 to WT+NASPM no washout; ‡‡‡p<0.001 to WT+NASPM washout; two-way ANOVA).

(D) Variable synaptic potentiation seen with NASPM washout after LTD induction in WT is prevented by PKA inhibition with H89 (5 μM), **(E)** by genetic disruption of PKA anchoring in ΔPKA mice, and **(F)** by genetic disruption of CaN anchoring in ΔPIX mice (t=70–80 min ***p<0.0001 to WT control; $^{\#\#\#}$p<0.0001 to WT+NASPM no washout; ‡‡‡p<0.001 to WT +NASPM washout; two-way ANOVA).

(G) Summary graph for LTD expression (%baseline) at t=80 min for experiments in panels A–F. *p<0.05, ***p<0.001 to respective pre-LTD values; $^{\#}$p<0.05, $^{\#\#}$p<0.01, $^{\#\#\#}$p<0.001 compared to WT control t=80 min; †p<0.05 to WT+NASPM no washout t=80 min; unpaired t-tests.

In all graphs data are mean ± SEM.

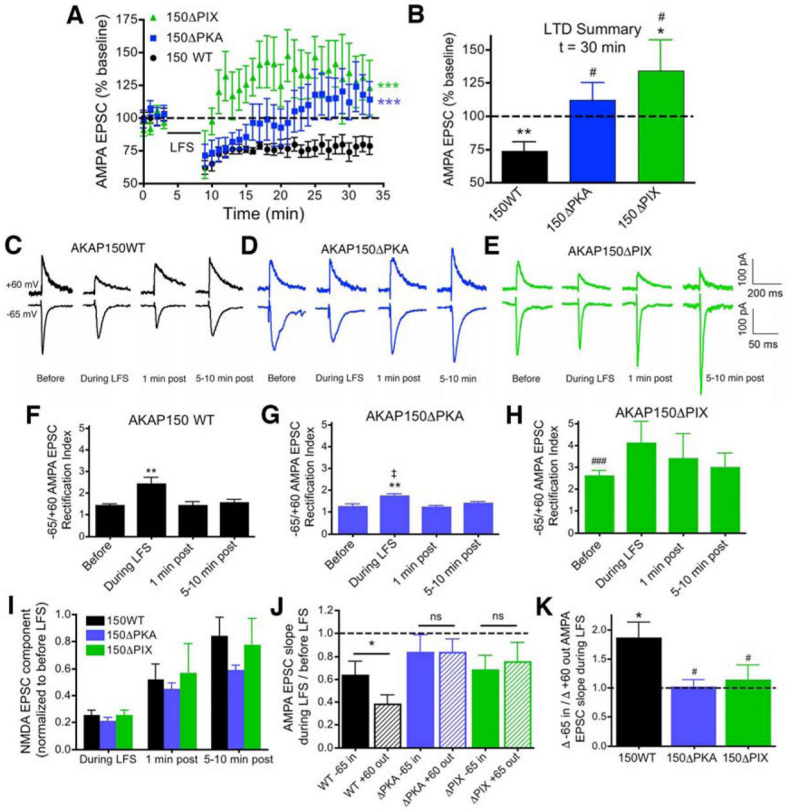

Figure 5. CP-AMPARs detected by increased inward rectification are transiently recruited to SC-CA1 synapses during LTD induction by AKAP150-PKA signaling and then are removed by AKAP150-CaN signaling

(**A**) Plots of AMPA EPSCs recorded in whole-cell configuration at −65 mV (normalized to % of baseline) over time showing that LTD expression is impaired in ΔPKA and ΔPIX compared to WT mice (***p<0.0001 two-way ANOVA to WT).

(**B**) Summary graph for LTD expression (%baseline) at t=30 min for experiments in panel A. *p<0.05, **p<0.01 to respective pre-LTD values; $^{\#}$p<0.05 to WT control t=30 min; unpaired t-tests.

(**C**) Representative outward (+60 mV) and inward (−65 mV) EPSCs recorded before, during, and at different times after LTD induction for WT, (**D**) ΔPKA, and (**E**) ΔPIX mice.

(**F**) Graphs of −65 mV/+60 mV AMPA EPSC RI revealing a prominent increase in AMPAR rectification in WT mice that is (**G**) greatly reduced in ΔPKA and (**H**) absent in ΔPIX mice, which already exhibit a basal increase in AMPAR RI. **p<0.01 by one-way ANOVA to respective before LTD values within genotype; ‡p<0.05 to WT during LFS; $^{\#\#\#}$p<0.001 to WT before LTD; unpaired t-tests.

(**I**) Graph of the outward NMDA EPSC component (+60 mV; measured 50 ms after peak) recorded during and after LTD induction (normalized to before values) in WT, ΔPKA, and ΔPIX mice.

(**J**) Graph of outward (+60 mV) and inward (−65 mV) AMPA EPSC slopes recorded during LFS induction of LTD (normalized to before values) in WT, ΔPKA, and ΔPIX mice. *p<0.05 to WT −65 in, paired t-test.

(**K**) Ratio of the changes (Δ) in inward (−65 mV)/outward (−60 mV) AMPA EPSC initial slope during LFS in WT, ΔPKA, and ΔPIX mice. *p<0.05 greater than 1.0 one-sample t-test; #p<0.05 one-way ANOVA to WT.
In all graphs data are mean ± SEM.

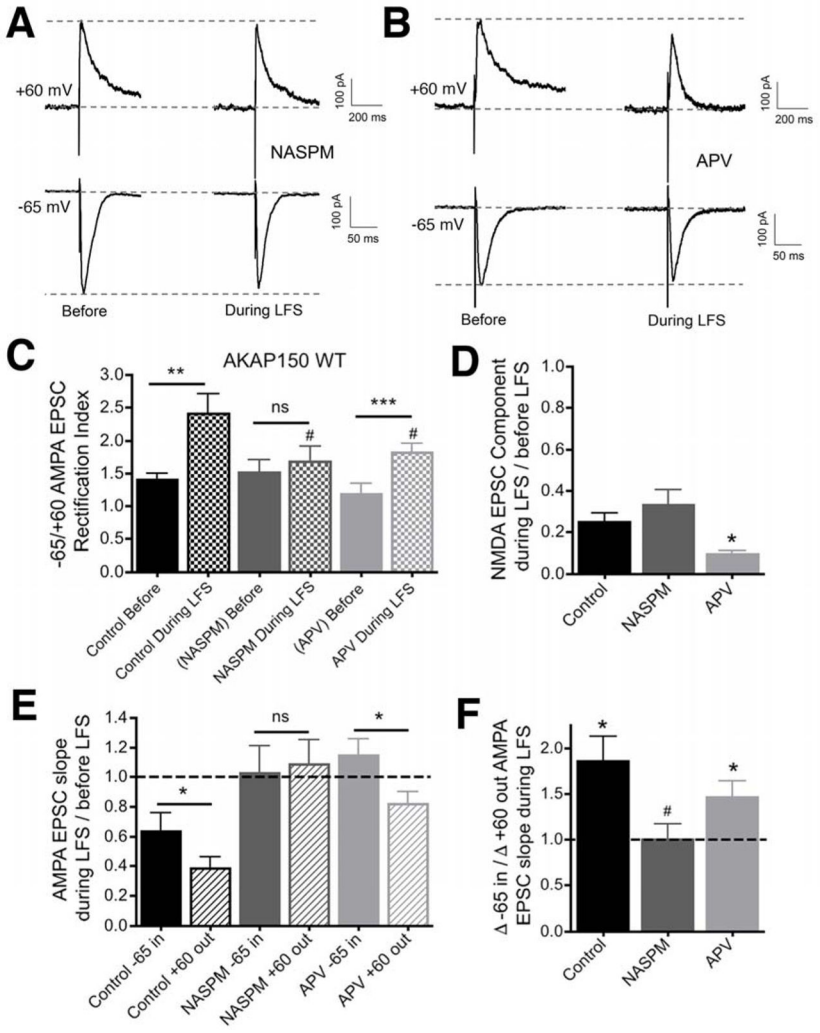

Figure 6. Increased synaptic AMPAR inward rectification during LTD induction at SC-CA1 synapses is blocked by CP-AMPAR antagonism

(**A**) Representative outward (+60 mV) and inward (−65 mV) EPSCs recorded before and during LFS-LTD induction for WT mice with acute application of NASPM or (**B**) APV during LFS. Note: NASPM and APV bath perfusion coincided with the onset of LFS, but due to time required for complete bath exchange, these antagonists likely did not reach final, effective concentrations until ~1 min. See also Figures S2 and S3.

(**C**) Graphs of −65 mV/+60 mV AMPA EPSC RI revealing that the increase in AMPA rectification during LFS in WT control mice (data from Figure 5F) is absent in NASPM and reduced in APV. **p<0.01, ***p<0.001 one-way ANOVA to respective before LTD values; $^{\#}$p<0.05 one-way ANOVA to Control during LFS.

(**D**) Graph of the outward NMDA EPSC component (+60 mV; measured 50 ms after peak) recorded during LTD induction (normalized to before values) in WT mice under control conditions (data from Figure 5I) and with acute application of NASPM or APV. *p<0.05 one-way ANOVA to both Control and NASPM.

(**E**) Graph of outward (+60 mV) and inward (−65 mV) AMPA EPSC slopes recorded during LFS induction of LTD (normalized to before values) in WT mice under control conditions (data from Figure 5J) and with acute application of NASPM or APV. *p<0.05 to WT −65 in paired t-test.

(**F**) Ratio of the changes (Δ) in inward (−65 mV)/outward (−60 mV) AMPA EPSC initial slope during LFS in WT mice under control conditions (data from Figure 5K) and with acute application of NASPM or APV. *p<0.05 greater than 1.0 by one-sample t-test; $^{\#}$p<0.05 one-way ANOVA to WT.

In all graphs data are mean ± SEM.

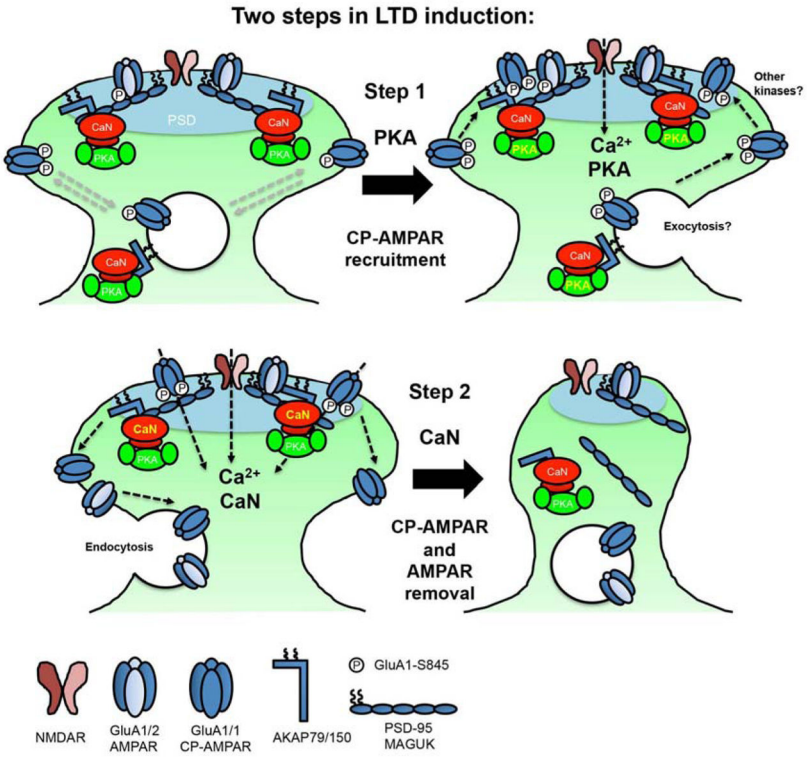

Figure 7. Model for CP-AMPAR signaling at hippocampal CA1 synapses during LTD

Two steps are necessary during LTD induction: 1) NMDAR Ca^{2+} influx and AKAP150-anchored PKA signaling rapidly recruit S845-phosphorylated GluA1/1 CP-AMPARs to the synapse and 2) CP-AMPARs are quickly removed from the synapse, along with GluA1/2 AMPARs, by CP-AMPAR and NMDAR Ca^{2+} influx activating AKAP150-anchored CaN signaling that also promotes GluA1 S845 dephosphorylation, spine shrinkage, and reduced postsynaptic localization of AKAP150 and PSD-95. CP-AMPAR synaptic recruitment could utilize pre-existing or newly delivered extrasynaptic receptors from recycling endosomes; AKAP150 is present at the PSD, extrasynaptic membrane, and recycling endosomes and thus could regulate CP-AMPARs in any or all of these locations. NMDAR activation of cAMP-PKA signaling may involve Ca^{2+}-activated adenylyl cyclases (not shown) that are known to bind to AKAP79/150.